BIOCHEMISTRY
including biophysical chemistry & molecular biology

Article

pubs.acs.org/biochemistry

The Unwound Portion Dividing Helix IV of NhaA Undergoes a Conformational Change at Physiological pH and Lines the Cation Passage

Abraham Rimon, Lena Kozachkov-Magrisso, and Etana Padan*

Department of Biological Chemistry, Alexander Silberman Institute of Life Sciences, Hebrew University, 91904 Jerusalem, Israel

ABSTRACT: pH and Na^+ homeostasis in all cells requires Na^+/H^+ antiporters. The crystal structure of NhaA, the main antiporter of *Escherichia coli*, has provided general insights into antiporter mechanisms and their pH regulation. Functional studies of NhaA in the membrane have yielded valuable information regarding its functionality in situ at physiological pH. Here, we Cys-scanned the discontinuous transmembrane segment (TM) IV (helices IVp and IVc connected by an extended chain) of NhaA to explore its functionality at physiological pH. We then tested the accessibility of the Cys replacements to the positively charged SH reagent [2-(trimethylammonium)ethyl] methanethiosulfonate bromide (MTSET) and the negatively charged 2-sulfonatoethyl methanethiosulfonate (MTSES) in intact cells at pH 8.5 and 6.5 and in parallel tested their accessibility to MTSET in high-pressure membranes at both pH values. We found that the outer membrane of *E. coli* TA16 acts as a partially permeable barrier to MTSET. Overcoming this technical problem, we revealed that (a) Cys replacement of the most conserved residues of TM IV strongly increases the apparent K_m of NhaA to both Na^+ and Li^+, (b) the cationic passage of NhaA at physiological pH is lined by the most conserved and functionally important residues of TM IV, and (c) a pH shift from 6.5 to 8.5 induces conformational changes in helix IVp and in the extended chain at physiological pH.

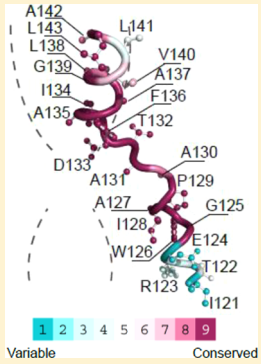

Living cells are critically dependent on processes that regulate intracellular pH, Na^+ content, and volume. Na^+/H^+ antiporters play a primary role in these homeostatic mechanisms (recently reviewed in refs 1−3). They are found in the cytoplasmic and organellar membranes of cells of many different origins, including plants, animals, and microorganisms. Moreover, they have long been human drug targets.[4]

NhaA, the principal Na^+/H^+ antiporter in *Escherichia coli*, is indispensable for adapting to high salinity, challenging Li^+ toxicity, and growing at alkaline pH (in the presence of Na^+).[2,5] It is widely spread in enterobacteria[1] and has orthologs throughout the biological kingdoms, including humans.[6]

Several biochemical characteristics of NhaA underpin its physiological roles: very high turnover,[7] electrogenicity with a 2:1 H^+:Na^+ stoichiometry[8] and strong pH dependence,[7] a property it shares with other prokaryotic[2,7] and eukaryotic Na^+/H^+ antiporters (reviewed in refs 4 and 9−13).

The recently determined crystal structure of downregulated NhaA crystallized at acidic pH[14] has provided the first structural insights into the antiport mechanism and pH regulation of a Na^+/H^+ antiporter.[3] NhaA consists of 12 transmembrane helices with their N- and C-termini on the cytoplasmic side of the membrane. A cytoplasmic funnel, lined by transmembrane segments (TMs) II, IX, IVc, and V, opens to the cytoplasm and ends in the middle of the membrane at the putative ion-binding site, where D164 of helix V is located[14] (Figure 1a); a periplasmic funnel, lined by TMs II, VIII, and XIp, opens into the periplasm and is separated from the cytoplasmic funnel by a group of densely packed hydrophobic residues.

The structure revealed a new fold in which TMs III, IV, and V are topologically inverted with respect to TMs X, XI, and XII. In each repeat, one TM (IV and XI, respectively) is interrupted by an extended chain in the middle of the membrane, leaving two short helices (IVc with IVp and XIc with XIp, respectively) oriented to the cytoplasm (c) or periplasm (p). This noncanonical TM assembly creates a delicately balanced electrostatic environment in the middle of the membrane at the ion-binding site(s), which likely plays a critical role in the cation exchange activity of the antiporter.[3,14]

Structures of other bacterial ion-coupled secondary transporters, which share little or no sequence homology, have since been determined. Remarkably, their structural fold also includes inverted topological repeats containing interrupted helices with functional implications similar to those for NhaA (reviewed in refs 15−17). Recently, the structure of a bacterial homologue of the bile acid sodium symporter, ASBT, was determined at 2.2 Å resolution. The overall architecture of this protein was very similar to that of NhaA, despite their lack of detectable sequence homology.[18] These proteins present the only two examples of interrupted helices crossing each other. The sodium-binding site near this crossing was identified in the ASBT homologue and predicted for NhaA,[18] in line with previous suggestions.[14]

Finally, the NhaA structure revealed its organization into two functional regions: (a) a cluster of amino acyl side chains that

Received: July 31, 2012
Revised: November 1, 2012
Published: November 6, 2012

ACS Publications © 2012 American Chemical Society

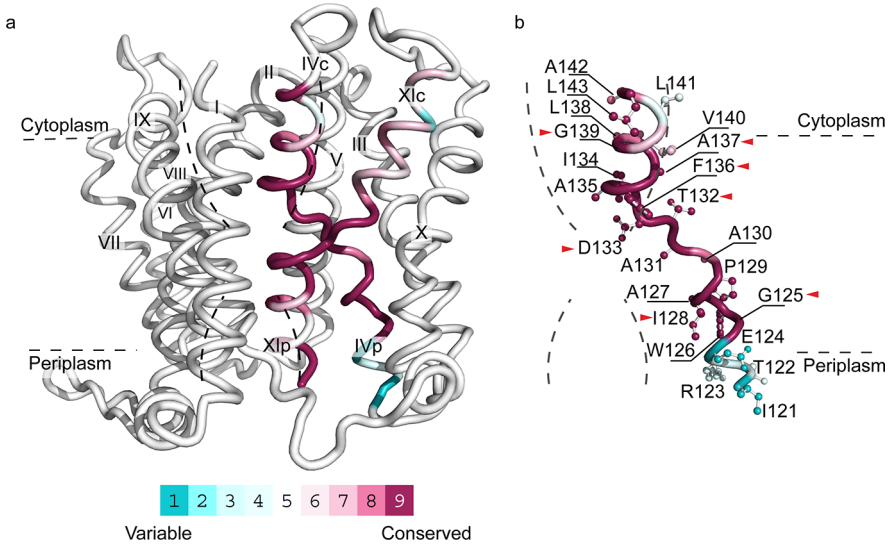

Figure 1. Architecture of TM IV and the cation funnels (cytoplasmic and periplasmic) in the crystal structure of NhaA at pH 4. (a) Crystal structure of helices comprising the cytoplasmic (TMs II, IVc, V, and IX) and periplasmic (TMs II, VIII, and XIp) funnels (black dashed lines) of NhaA and the TM assembly (TMs IV and IX) (colored as in panel b) shown in ribbon representation viewed parallel to the membrane (gray dashed lines). (b) TM IV is shown colored according to its evolutionary conservation using Consurf (http://consurf.tau.ac.il/). The color-coding bar indicates the degree of residue variability (from 1 for most variable to 9 for most conserved). The residues on TM IV that replaced Cys are labeled in black and shown in ball-and-stick configuration. Cys replacements affecting the apparent K_m for Na^+ and Li^+ are denoted with red arrowheads. The figures were generated using PyMOL (http://pymol.sourceforge.net/).

are involved in pH regulation, termed "pH sensor" (residues on loops VIII and IX and TMs IX, IVc, and II), and (b) a catalytic region containing the ion-binding sites (residues on TMs IV and V) that is ~9 Å from the pH sensor. A unique role has been ascribed to D133 of TM IV in NhaA's pH response.[19]

The structure of the acid-locked downregulated conformation of NhaA has thus revealed that TM IV is part of a most unique fold of NhaA that lines the cytoplasmic funnel and contributes to the active site; residues on TM IV have been predicted to participate in the functionality and pH regulation of NhaA. However, the structure was determined at pH 4 when NhaA was downregulated;[14] NhaA is activated at pH 6.5 and reaches maximal activity at pH 8.5.[7] As a result, the structure of the active conformation(s), the process(es) leading to it, and the residues participating in it have remained elusive. Hence, we undertook a study of TM IV, which is both structural and functional, in the membrane when NhaA is active, i.e., at physiological pH. Our results reveal amino acid residues in TM IV participating in the cation passage and pH regulation of NhaA, and a pH-induced conformational change in TM IV.

MATERIALS AND METHODS

Bacterial Strains and Culture Conditions. EP432 is an *E. coli* K-12 derivative, which is *mel*BLid, Δ*nha*A1::*kan*, Δ*nha*B1::*cat*, Δ*lac*ZY, *thr*1.[5] TA16 is *nha*A$^+$*nha*B$^+$*lac*I^Q and otherwise isogenic to EP432.[7] Cells were grown in either L broth (LB) or modified L broth (LBK[20]). Where indicated, the medium was buffered with 60 mM 1,3-bis{tris(hydroxymethyl)-methylamino}propane (BTP). For plates, 1.5% agar was used. For induction, the cells were also grown in minimal medium A[21] without sodium citrate and with 0.5% (w/v) glycerol, 0.01% (w/v) $MgSO_4 \cdot 7H_2O$, and 2.5 μg/mL thiamine. The antibiotic used was 100 μg/mL ampicillin or 50 μg/mL kanamycin. To test the resistance to Li^+ and Na^+, EP432 cells transformed with the respective plasmids were grown on LBK to an OD_{600} of 0.5. Samples (2 μL) of serial 10-fold dilutions of the cultures were spotted onto agar plates containing the indicated concentrations of NaCl or LiCl at the various pHs and incubated for 48 h at 37 °C.

Plasmid. pCL-AXH3 is a derivative of pCL-AXH2[22] and contains a silent BstXI site at position 248 in *nha*A.

Site-Directed Mutagenesis. Site-directed mutagenesis was conducted following a polymerase chain reaction-based protocol[23] or mediated by DpnI.[24] The mutations were created using plasmid pCL-AXH3 as the template. Mutants A118C and S246C were constructed as described in ref 25 and mutant H225C as described in ref 26. All mutations were verified by DNA sequencing of the entire gene through the ligation junction with the vector plasmid.

Isolation of Everted Membrane Vesicles and Assay of Na^+/H^+ Antiporter Activity. Everted vesicles from EP432 cells transformed with the respective plasmids were prepared as previously described[27,28] and used to determine Na^+/H^+ or Li^+/H^+ antiporter activity.[27,28] The antiporter activity assay was based on the measurement of Na^+- or Li^+-induced changes in the ΔpH as measured by acridine orange, a fluorescent probe of ΔpH. The fluorescence assay was performed in a 2.5 mL reaction mixture containing 50−100 μg of membrane protein, 0.5 μM acridine orange, 150 mM KCl, 50 mM BTP, and 5 mM $MgCl_2$, and the pH was titrated with HCl. After energization with D-lactate (2 mM), fluorescence was quenched to achieve a steady state, and then 10 mM Na^+ or Li^+ was added. A reversal of the fluorescence level (dequenching) indicates that protons are exiting the vesicles during antiport with either Na^+ or Li^+. As shown previously, the end level of dequenching is a good estimate of antiporter activity,[29] and the ion concentration that gives half-maximal dequenching is a good estimate of the apparent K_m of the antiporter.[29,30] The concentration range of the tested cations was 0.01−100 mM at the indicated pHs, and the apparent K_m values were calculated by linear regression of a Lineweaver−Burk plot.

dx.doi.org/10.1021/bi301030x | *Biochemistry* 2012, 51, 9560−9569

Table 1. Single-Cys Replacements in TM IV of NhaA[a]

mutation	expression (% of WT)[b]	growth[c]			activity (maximal dequenching %)[d]		apparent K_m (mM)[e]	
		Na^+ (7)	Na^+ (8.3)	Li^+ (7)	Na^+	Li^+	Na^+	Li^+
T122C	98	+++	+++	+++	83	82	0.44	0.06
R123C	95	+++	−	+++	ND	ND	ND	ND
E124C	94	+++	+++	+++	ND	ND	ND	ND
G125C[f]	30	+++	−	+++	16	74	12	0.56
W126C	98	+++	+++	+++	86	83	0.32	0.04
A127C[g]	92	+++	+++	+++	88	85	0.24	0.02
I128C	90	+++	++	+++	75	75	0.58	0.13
P129C[g]	99	+++	+++	+++	98	94	0.40	0.03
A130C	95	+++	+++	+++	97	94	0.50	0.03
A131C	81	+++	+++	+++	85	83	0.43	0.07
T132C[g]	95	+++	+++	+++	62	82	12.40	0.70
D133C[g]	40	+++	+++	+++	62	68	3.60	1.24
I134C	100	+++	+++	+++	78 80	0.80	0.07	
A135C	ND	ND	ND	ND	ND	ND	ND	ND
F136C[f]	100	++	−	−	1	0	102	ND
A137C[f]	100	+++	+++	+++	41	79	7.20	0.8
L138C	118	+++	+++	+++	90	90	0.11	0.03
G139C	83	+++	+	+++	73	80	0.77	0.39
V140C	50	+++	+++	+++	83	73	0.38	0.80
L141C	ND	ND	ND	ND	ND	ND	ND	ND
A142C	76	+++	+++	+++	90	90	0.17	0.04
pCL-AXH3 (control)	100	+++	+++	+++	98	94	0.19	0.02
pBR322 (negative control)	−	−	−	−	−	−	−	−

[a]For characterization of the mutations, EP432 cells transformed with the plasmids carrying the indicated mutations were used. [b]Expression level expressed as a percentage of that of control cells (EP432/pCL-AXH3) expressing CL-NhaA. [c]Growth experiments were conducted at 37 °C on LB-modified agar plates containing 0.6 M NaCl at pH 7 or 8.3 or 0.1 M LiCl at pH 7: +++, number and size of the colonies after incubation of the control for 48 h; ++, same number of colonies as the control but smaller in size; +, both size and number of colonies reduced compared to those of controls; −, no growth. [d]Na^+/H^+ and Li^+/H^+ antiporter activity at pH 8.5 determined with 10 mM NaCl or LiCl. Activity expressed as the percentage of dequenching. EP432/pBR322 served as a negative control. [e]The apparent K_m for the ions was determined at pH 8.5, as described in Materials and Methods. [f]Data taken from ref 34. [g]Data taken from ref 22.

Isolation of High-Pressure Membranes. TA16 cells transformed with the NhaA Cys replacement variants were grown and induced and their membranes isolated in a French press as for isolation of the everted membrane vesicles,[27,28] except that the pressure for cell breakage was higher (20000 psi).

Detection and Quantitation of NhaA and Its Mutated Derivatives in the Membrane. The total membrane protein was determined according to the method described by Bradford.[31] We determined the expression level of His-tagged NhaA mutants by resolving the Ni-NTA-purified proteins by sodium dodecyl sulfate−polyacrylamide gel electrophoresis (SDS−PAGE), staining the gels with Coomassie blue, and quantifying the band densities with Image Gauge (Fuji).[32]

Accessibility to Membrane-Impermeant Sulfhydryl Reagents MTSES and MTSET in Intact Cells. TA16 cells transformed with the plasmids expressing the respective variants were grown in minimal medium A to an OD_{600} of 0.7 and induced by addition of 0.5 mM isopropyl thiogalactoside (IPTG) for 2 h (to an OD_{600} of 1.1). Then the cells were washed and concentrated 10 times in 1 mL of KP_i buffer containing 100 mM potassium phosphate and 5 mM $MgSO_4$ at the indicated pHs and incubated for 30 min with 10 mM sulfhydryl (SH) reagent at 23 °C while being shaken slightly (450 rpm). The reaction was stopped by rapid centrifugation (10000*g*), and the mixture was diluted in 40 mL of KP_i buffer at the respective pHs and recentrifuged. The cells were washed twice, resuspended in 1 mL of KP_i buffer, and sonicated (three times for 10 s each at 4 °C, Vebra Cell model VCX 750). Unbroken cells were removed by centrifugation (10000*g*) and the membranes collected by centrifugation (Beckman, TLA 100.4, 265000*g* for 30 min at 4 °C); the membranes were then resuspended in 0.5 mL of TSC buffer [10 mM Tris (pH 7.5), 250 mM sucrose, and 140 mM choline chloride]. The protein was extracted and affinity-purified on Ni^{2+}-NTA (Qiagen) and left bound on the beads. The beads were washed twice in binding buffer[32] at pH 7.4, washed in 500 μL of SDS−urea buffer [6 M urea, 20 mM Tris (pH 7.5), 2% (w/v) SDS, and 500 mM NaCl], resuspended in 100 μL of SDS−urea buffer containing 0.5 mM fluorescein 5-maleimide (Molecular Probes), further incubated for 30 min at 23 °C, and washed in SDS−urea buffer to determine the amount of free Cys remaining after treatment with 2-sulfonatoethyl methanethiosulfonate (MTSES) or [2-(trimethylammonium)ethyl] methanethiosulfonate bromide (MTSET). Then the beads were washed with 1 mL of SDS−urea buffer, and the protein was eluted in sample buffer containing 300 mM imidazole (without reducing agent) and separated by SDS−PAGE. For the evaluation of fluorescence intensity, the gels were photographed under UV light (260 nm) as described previously.[25] To quantify the amount of protein, the gels were stained with Coomassie blue and the density of the bands was determined. After normalization of the fluorescence intensity to the amount of protein in the band, the accessibility to MTSES or MTSET was determined from the difference in the fluorescence of the reagent-treated versus untreated samples (100% fluorescence =

dx.doi.org/10.1021/bi301030x | Biochemistry 2012, 51, 9560−9569

0% accessibility[25]). The standard deviation was between 5 and 10%.

MTSET Accessibility Test with High-Pressure Membranes. The frozen stored membranes were washed in a reaction mixture containing 150 mM choline chloride, 50 mM BTP, and 5 mM $MgCl_2$ (pH 6.5 or 8.5) and resuspended, yielding 1 mg of membrane protein in 0.5 mL of the reaction mixture. Following addition of MTSET, the reaction mixture was sonicated (Sonics Vibra Cell, 750 W from Sonics&Materials) twice for 20 s each time, incubated, and processed as described above for intact cells.

RESULTS

The crystal structure of NhaA at pH 4[14] shows the noncanonical structure of TM IV; it is divided by an extended chain into two small helices: IVp and IVc (panels a and b of Figure 1, respectively). The N-terminus of helix IVp (I121) connects loops III and IV in the periplasm so that like the loop, helix stretch I121−E124 is located in the periplasm. The rest of helix IVp (G125−A131) is packed inside the NhaA molecule along the periplasmic funnel and is connected by its C-terminus (A131) to an extended chain (T132 and D133). The extended chain connects helix IVc (I134−L143) that lines the cytoplasmic funnel. The cytoplasmic end of TM IV (L141−L143) connects loops IV and V. We studied the structure−function relationships in TM IV.

Construction of Cys-Replacement Mutations in TM IV. To search for functionally important residues on TM IV, each of its amino acids was replaced with Cys in Cys-less NhaA (CL-NhaA in plasmid pCL-AXH3), a variant that is as strongly expressed and active as native NhaA.[32] NhaA mutations G125C, F136C, A137C, P129C, T132C, and D133C, which had been previously isolated on a different plasmid,[22] were transferred to pCL-AXH3 to avoid effects of different vector plasmids.

Cys-Replacement Mutants of TM IV, Expression in the Membrane, and Growth Phenotypes. To characterize the NhaA variants with respect to expression, growth, and antiporter activity (Table 1), the mutated plasmids were transformed into EP432,[5] an *E. coli* strain that lacks the two Na^+-specific antiporters (NhaA and NhaB). This strain does not grow on selective media (0.6 M NaCl at pH 7 or 8.3 or 0.1 M LiCl at pH 7.0), nor does it exhibit Na^+/H^+ antiporter activity in isolated everted membrane vesicles, unless it is transformed with a plasmid encoding an active antiporter (reviewed in ref 2).

All variants were significantly (≥30%) expressed as compared to the expression level of the wild type [100% (Table 1)]. Notably, because all variants were expressed from multicopy plasmids, even the low level of expression was far above the level expressed from a single chromosomal gene that confers a Na^+-resistance phenotype.[33]

Most variants grew like the wild type on the selective agar plates (Table 1). Variants R123C, G125C, I128C, and G139C grew like the wild type on the NaCl and LiCl selective media at neutral pH, but on the NaCl selective medium at alkaline pH, variant G139C grew slowly and R123C and G125C did not grow (Table 1). Variant F136C grew slowly and then only on the NaCl selective medium at neutral pH.

Effect of Cys-Replacement Mutations in TM IV on Na^+/H^+ and Li^+/H^+ Antiporter Activity. Cys replacements G125C, T132C, D133C, F136C, and A137C have previously been found to be important for NhaA ion-exchange activity, and variant G125C showed an additional effect on pH regulation (Table 1 and refs 22 and 34). These Cys replacements were further studied here.

The variants' Na^+/H^+ and Li^+/H^+ antiport activities were measured in everted membrane vesicles isolated from EP432 transformed with plasmid pCL-AXH3 encoding the respective variants. The activity was estimated from the change caused by either Na^+ or Li^+ to the ΔpH maintained across the membrane, as measured by acridine orange, a fluorescent probe of ΔpH. EP432 transformed with plasmid pCL-AXH3 encoding CL-NhaA or vector plasmid pBR322 served as a positive or negative control, respectively (Figure 2 and Table 1). The

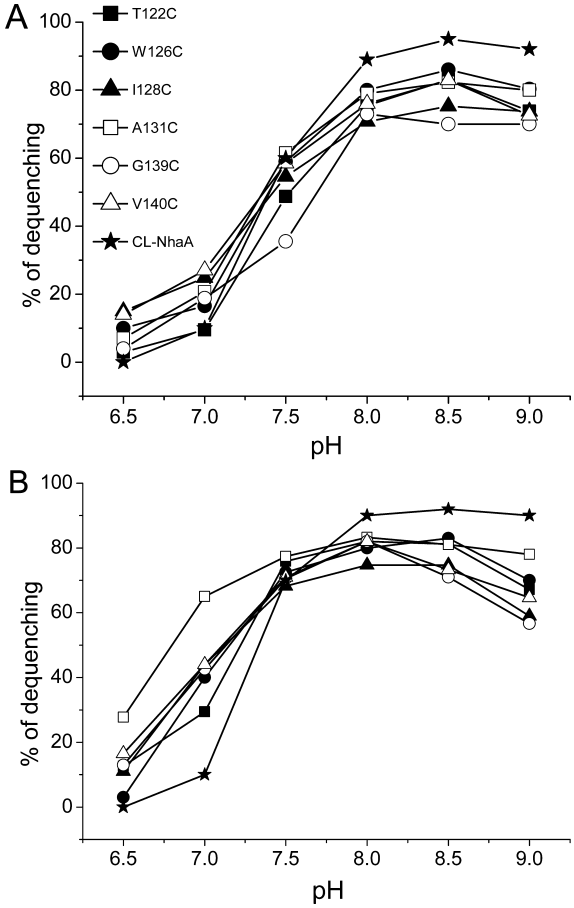

Figure 2. Na^+/H^+ antiporter activity in everted membrane vesicles of Cys replacements in NhaA TM IV. Everted membrane vesicles were prepared from EP432 cells expressing the indicated NhaA variants and grown in LBK (pH 7). The Na^+/H^+ and Li^+/H^+ antiporter activities were determined in the presence of (A) 10 mM NaCl or (B) 10 mM LiCl at the indicated pH values, using acridine orange fluorescence to monitor ΔpH. Results are expressed as the percent dequenching of the fluorescence due to cation addition. All experiments were repeated at least three times with nearly identical results.

apparent K_m values for Na^+ and Li^+ at pH 8.5 and the extent of activity (maximal dequenching) at pH 8.5 were determined for each mutant (Table 1 and data not shown). Many Cys replacements showed several-fold increases in the apparent K_m for Na^+ and Li^+: G125C, 63- and 28-fold; I128C, 3- and 6.5-fold; T132C, 65- and 35-fold; D133C, 18- and 62-fold; F136C, 536-fold (for Na^+); A137C, 37- and 40-fold; G139C, 4- and 20-fold; V140C, 2- and 40-fold. These results explain the slower growth or the lack of growth of several variants under selective

dx.doi.org/10.1021/bi301030x | *Biochemistry* 2012, 51, 9560−9569

conditions with respect to Na^+ and Li^+ (G125C, I128C, F136C, and G139C in Table 1). However, the growth phenotype cannot always be explained on the basis of the K_m (variant I132C is an example). The mutation might affect other unknown parameters.

We have previously shown[22,34] that when measured at saturating concentrations of Na^+, NhaA variants with mutations that affect the apparent K_m but not the pH dependence show a pH dependence very similar to that of the wild type at a saturating concentration of the substrate. In contrast, variants with mutations that affect both the apparent K_m and the pH dependence of the antiporter retain the abnormal pH dependence, even at saturating ion concentrations. We therefore measured the effect of Na^+ concentration (10 mM vs 100 mM) on the pH dependence of the variants' activity. Most variants (Figure 2A), including T132C and D133C,[22,34] were of the first type. Two variants in helix IVc showed an effect on pH regulation, G125C[34] in the presence of Na^+ and A131C, which was tested here in the presence of 10 mM Li^+ (Figure 2B) and 100 mM Li^+ (data not shown) with identical results.

MTSET Accessibility Test with the Cys-Replacement Variants in TM IV at pH 8.5 and 6.5 in Intact Cells (from the periplasmic side of the membrane). To determine whether TM IV residues line the cation passage at physiological pH, we tested the accessibility of the Cys replacements to the SH reagents MTSET and MTSES at pH 8.5, when NhaA is fully active, or at pH 6.5, when NhaA is downregulated.[7] These SH reagents are water-soluble, membrane-impermeant, and positively and negatively charged, respectively,[35,36] and have a diameter quite similar to that of hydrated Na^+ (7.2 Å); MTSET is ~11.5 Å long and 6 Å wide. As a result, MTSET and MTSES can reach the Cys replacements exposed directly to the reaction medium or via water-filled funnels in the protein connected to the reaction medium.

The accessibility of the TM IV Cys replacements to MTSET (Figure 3) or MTSES (Figure 4) was first tested in intact cells (from the periplasmic side of the membrane). The procedures were identical with both reagents (see Materials and Methods) and are reiterated briefly here for the MTSET treatment. Intact cells were incubated with MTSET at pH 8.5 or 6.5. Then NhaA was affinity-purified on Ni^{2+}-NTA beads, left bound to the beads, denatured, and treated with fluorescein maleimide, a fluorescent SH reagent. This reagent has previously been shown to bind any free Cys in purified NhaA protein and not to bind to CL-NhaA.[25] The proteins of the MTSET-treated samples at pH 8.5 or 6.5 were separated by SDS–PAGE. The level of fluorescence (Figure 3A, top panel) and the amount of protein on the gels (Figure 3A, bottom panel) were monitored in the MTSET-treated samples at pH 8.5 (Figure 3A, lane c) or pH 6.5 (Figure 3A, lane b). The fluorescence intensity was normalized to the amount of the respective protein. For each variant, an untreated control was processed in parallel (Figure 3, lane a), and its fluorescence level was set at 100% (0% accessibility) to allow expression of MTSET accessibility in percent (Figure 3B). We scored ≥10% accessibility as positive.[25] Variant H225C,[32,37] located at the periplasmic end of TM VIII (Figure 3A), and variant A118C,[25] located in the III–IV loop (data not shown), served as positive controls.

The crystal structure at pH 4[14] shows that residues T122C–E124C at the periplasmic end of helix IVp protrude into the periplasm (Figures 1 and 3C). In line with the crystal structure, the test of MTSET accessibility at pH 8.5 (Figure 3A, lane c,

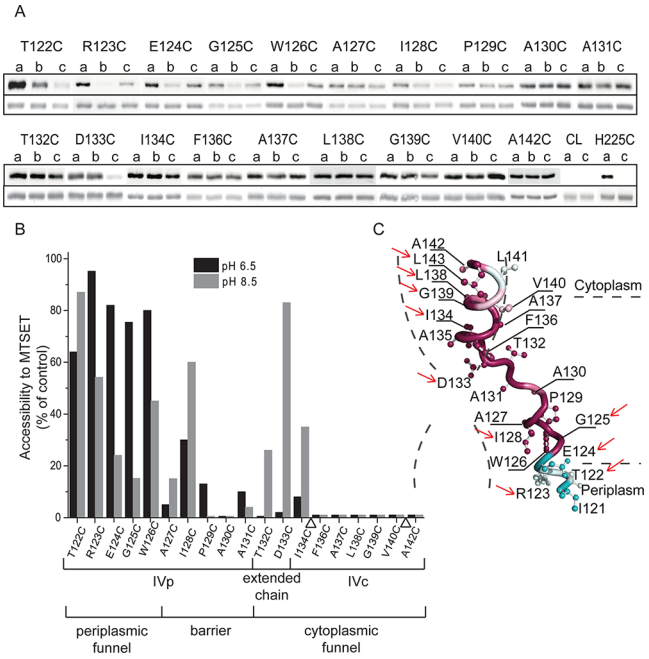

Figure 3. Accessibility of Cys replacements in TM IV to MTSET in intact cells at pH 6.5 and 8.5. Intact cells expressing the Cys-replacement mutants in TM IV of Cys-less NhaA were incubated with MTSET at pH 6.5 and 8.5. Proteins were purified by Ni^{2+}-NTA affinity chromatography and labeled on the beads with fluorescein maleimide to estimate the percentage of free Cys remaining. (A) Eluted proteins were resolved by SDS–PAGE, and the fluorescence level was monitored and photographed under UV light (top). The gel was stained with Coomassie blue and photographed under ordinary light to assess the protein concentration (bottom). Three samples were run for each variant: (a) nontreated control, (b) MTSET-treated sample at pH 6.5, and (c) MTSET-treated sample at pH 8.5. (B) Fluorescence intensity normalized to the respective protein concentration and expressed as percent fluorescence intensity of the untreated control. Accessibility to MTSET = 100% − % fluorescence intensity of the treated sample. The standard deviation was between 5 and 10%. Triangles denote Cys replacements that were not studied. (C) Crystal structure of TM IV shown as in Figure 1b. Arrows indicate the residues with Cys replacements that are accessible to MTSET in both intact cells and high-pressure membranes (Figure 5).

and Figure 3B) showed that these Cys replacements are accessible to MTSET from the periplasmic side of the membrane in intact cells at pH 8.5. However, the closer the residue to the membrane, the lower the MTSET accessibility; i.e., T122C was 88% accessible and R123C 55% accessible, whereas E124C at the membrane border was only slightly (25%) accessible and G125C, located in the membrane interface, barely (15%) accessible (Figure 3B). Surprisingly, the results of the accessibility test of TM IV with MTSET in intact cells at pH 6.5 were very different (Figure 3A, lane b, and Figure 3B). An acidic pH dramatically increased the accessibility of MTSET to residues T122C–G125C, and the reduction in accessibility with a decreased distance from the membrane seen at pH 8.5 disappeared at pH 6.5.

According to the crystal structure at pH 4,[14] the remaining stretch of α-helix IVp (W126C–A131C) is in the membrane and comprises ~1.5 helical turns (Figures 1 and 3C). In line with the crystal structure, the MTSET accessibility test at pH 8.5 showed two peaks of accessibility, ~1.5 helix turns apart (Figure 3B); the MTSET accessibility increased at W126C (48%), decreased at A127C (14%), and then increased again at

dx.doi.org/10.1021/bi301030x | Biochemistry 2012, 51, 9560–9569

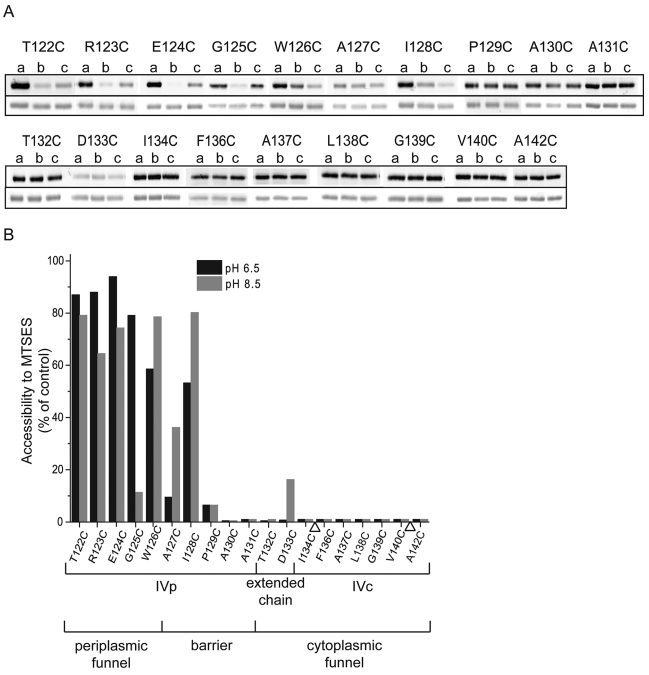

Figure 4. Accessibility of Cys replacements in TM IV to MTSES in intact cells at pH 6.5 and 8.5. Intact cells expressing the indicated variant were incubated with MTSES at different pH values (6.5 and 8.5) and processed as described in the legend of Figure 3. Triangles denote Cys replacements that were not studied. Three samples were run for each variant: (a) nontreated control, (b) MTSET-treated sample at pH 6.5, and (c) MTSET-treated sample at pH 8.5.

I128C (60%), followed by insignificant accessibility (<5%) at P129C−A131C, the C-terminus of helix IVp. The accessibility test at acidic pH for residues W126C−A131C showed the same pattern of accessibility as at alkaline pH, but the percentage of accessibility of Cys replacements A127C−A131C was markedly reduced (Figure 3B).

The extended chain connecting helix IVp to helix IVc lines the bottom of the cytoplasmic funnel and is separated from the periplasmic funnel by a hydrophobic barrier, according to the pH 4 crystal structure[14] (Figures 1 and 3C). A dramatic increase in MTSET accessibility was observed at pH 8.5 at the extended chain and the N-terminus of helix IVc (T132C−I134C): T132C (30%), D133C (88%), and I134C (35%). In marked contrast, at pH 6.5, the accessibility of MTSET to T132C−D133C almost totally disappeared (Figure 3B).

Finally, as predicted by the pH 4 crystal structure[14] (Figure 3C), most residues of helix IVc (A135C−A142C), which line the cytoplasmic funnel, were completely inaccessible to MTSET in intact cells (from the periplasmic side of the membrane) at both pH 8.5 and 6.5 (Figure 3B).

MTSES Accessibility Test with the Cys-Replacement Variants in TM IV at pH 8.5 and 6.5 in Intact Cells. In general, the pattern of accessibility of MTSES to Cys replacements T122C−P129C in NhaA TM IVp in intact cells was similar to that of MTSET, at pH 6.5 and 8.5 (panels A and B of Figures 4 and 3, respectively), but the percentage of MTSES accessibility was higher than that of MTSET. Beyond P129C, none of the Cys replacements, including the extended chain and helix IVc, showed MTSES accessibility at either pH, except for D133C, which showed very low MTSES accessibility (15%).

In summary, there was a major difference between the accessibility of MTSET and MTSES to Cys replacements of TM IV. MTSET penetrated deeper into the NhaA molecule in intact cells than MTSES (compare Figures 3B and 4B). Furthermore, an acidic pH increased the accessibility of residues at helix IVp (Figures 3B and 4B), but an alkaline pH dramatically increased the accessibility at the extended chain.

MTSET Accessibility Test with the Cys-Replacement Variants of TM IV in High-Pressure Membranes (from both sides of the membrane). The results of the MTSET versus MTSES accessibility test in intact cells were most surprising, mainly the opposite effect of pH on the accessibility of residues in helix IVp and in the extended chain (Figures 3B and 4B). We therefore considered the possibility that the outer membrane is a permeability barrier to MTSET and MTSES, which is more pronounced at alkaline pH than at acidic pH in intact cells. We tested the accessibility of Cys replacements in TM IV to MTSET in membrane vesicles isolated at high pressure and sonicated in the presence of MTSET before incubation with MTSET (Figure 5). This membrane fraction (termed high-pressure membranes) is devoid of outer membrane and periplasm and includes a mixture of right-side-out and inside-out vesicles of the cytoplasmic membrane. Hence, reagents that are soluble in the medium can access each TM IV Cys replacement exposed to the reaction medium.

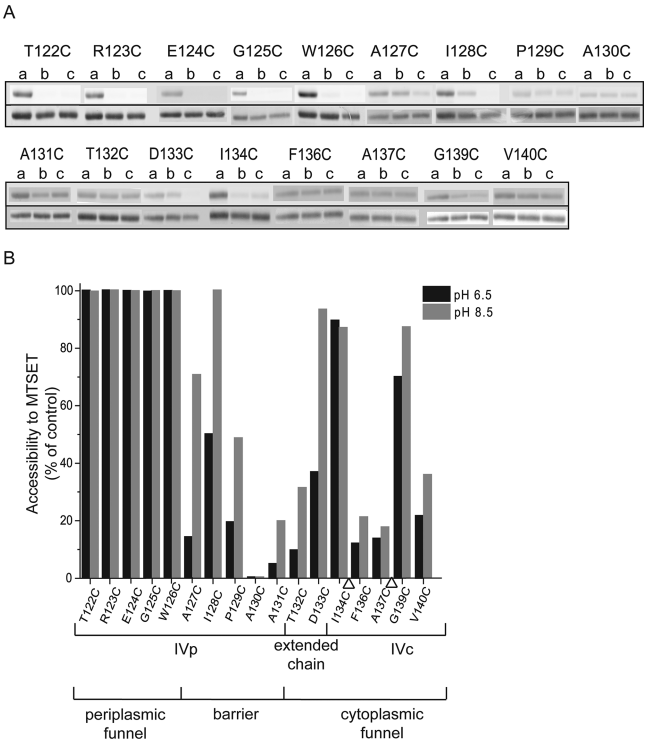

Figure 5. Accessibility of Cys replacements in TM IV to MTSET in high-pressure membranes at pH 6.5 and 8.5. High-pressure membranes were isolated from cells expressing the Cys-replacement variants and incubated with MTSET at pH 6.5 and 8.5 as described in Materials and Methods. Then, the proteins were isolated and processed as described in the legend of Figure 3. The standard deviation was between 5 and 10%. Triangles denote Cys replacements that were not studied. Three samples were run for each variant: (a) nontreated control, (b) MTSET-treated sample at pH 6.5, and (c) MTSET-treated sample at pH 8.5.

dx.doi.org/10.1021/bi301030x | Biochemistry 2012, 51, 9560−9569

Indeed, once the outer membrane was removed, stretch T122C−W126C of helix IVp, which is located in or near the periplasm (Figure 1b), became fully accessible to MTSET (100%) at pH 6.5 and 8.5 (Figure 5A,B). These results imply that the outer membrane serves as a permeability barrier to MTSET, more so at alkaline pH than at acidic pH. Further toward the cytoplasm (A127C−I134C), the pattern of accessibility observed in the high-pressure membranes was very similar to that observed in intact cells (compare Figures 3B and 5B), but MTSET accessibility was higher in the high-pressure membranes because of the absence of an outer membrane. Furthermore, both experimental systems showed that the accessibility of MTSET to Cys replacements in this NhaA stretch is higher at alkaline than at acidic pH (Figure 5, for example, D133C). These results strongly suggest that in addition to the permeability of the outer membrane, MTSET accessibility is controlled by pH. Finally, the Cys replacements lining the cytoplasmic funnel, I134C−V140C, which were not at all accessible from the periplasm in intact cells at either pH, became exposed in the high-pressure membranes and showed a large peak at G139C, the magnitude of which was also slightly increased at alkaline pH (Figure 5). Taken together, the MTSET accessibility test with high-pressure membranes revealed Cys replacements in NhaA TM IV that are accessible to the medium at physiological pH, and the strong pH dependency of the accessibility of MTSET to several of the residues, mainly in TM IVp and the extended chain.

DISCUSSION

Cys scanning of the discontinuous NhaA TM IV (helices IVp and IVc connected by an extended chain) and testing the accessibility, in intact cells, of the Cys replacements to the positively (MTSET) and negatively (MTSES) charged SH reagents, at pH 8.5 and 6.5, as well as the accessibility to MTSET in high-pressure membranes at both pHs, we learned that the outer membrane of *E. coli* TA16 is a partial permeability barrier to MTSET and revealed the following. (a) Similar to the acidic pH crystal structure,[14] the cation passage of NhaA at physiological pH is the most evolutionarily conserved segment of NhaA and involves cytoplasmic and periplasmic funnels lined by helix IVc and helix IVp, respectively. In marked contrast to the helices, the extended chain is buried at acidic pH and exposed to the periplasm at physiological pH. (b) Cys replacement of the most conserved residues in the extended chain and in helices IVp and IVc increases the apparent K_m of NhaA to both Na^+ and Li^+, and two Cys replacements (in helix IVp) also affect NhaA's pH response. (c) There is a marked pH-induced conformational change in the extended chain and helix IVp at physiological pH.

The Outer Membrane of *E. coli* TA16 Is a Partial Permeability Barrier to MTSET in Intact Cells. As exemplified by NhaA[32] and other transport proteins (reviewed in ref 38), in situ functional studies of Cys replacements have yielded important information about the expression, growth, and membrane phenotypes of genetic variants. Furthermore, the availability of a single Cys in CL proteins has allowed the application of various SH reagents to probe the proteins, site-specifically, for different properties. A test of the accessibility of CL-NhaA Cys replacements to membrane-impermeant probes identified locations on NhaA that are exposed to water-filled areas. The accessibility tests conducted as a function of pH revealed pH-induced conformational changes.[39] Here we applied these approaches along with the critical controls to show that CL-NhaA is not affected by the reagents,[25,40] the effect of pH on the rate of chemical modification of the SH groups is minimal,[41] and all Cys replacements in the denatured protein react with the reagents.[41] However, when using intact cells and high-pressure membranes in parallel for the MTSET accessibility test with Cys replacements in NhaA TM IV, we came upon a previously unrecognized technical problem: the outer membrane is a partial permeability barrier to MTSET, resulting in biased accessibility information from intact cells. In intact cells, a SH reagent that can freely permeate the outer membrane accesses the cytoplasmic membrane only from the periplasm and therefore identifies NhaA Cys replacements that are located in or are facing the periplasm, or are connected to it by water-filled funnels. In high-pressure membranes prepared in the presence of the reagent, where the outer membrane is removed, the orientation of the cytoplasmic membrane is a mixture of right-side-out and inside-out membrane vesicles. Hence, the reagent accesses and identifies NhaA Cys replacements that are exposed either directly or indirectly to both the cytoplasm and the periplasm. Therefore, the accessibility of MTSET to residues located inside the periplasm (away from the cytoplasmic membrane) should be equal in both experimental systems.

According to the crystal structure at pH 4, such residues are T122C−G125C of NhaA helix IVp (Figures 1 and 3B,C), and assuming that their structure is unchanged at physiological pH, they should show similar accessibility in both experimental systems. However, a comparison of Figures 3B and 5B shows that whereas the accessibility of MTSET to residues T122C−G125C in high-pressure membranes is equal and maximal (100%) at both pH 6.5 and 8.5 (Figure 5), the accessibility of these residues in intact cells at pH 6.5 is slightly lower (~80%) and at pH 8.5 only T122C is highly accessible; the accessibility of the other Cys replacements decreases with their distance from the membrane (Figure 3B). It is therefore highly likely that the outer membrane of *E. coli* TA16 is a partial permeability barrier to MTSET, more so at pH 8.5 than at pH 6.5. In support of this, the level of accessibility of Cys replacements in the rest of TM IV (G125C−A142C) in the high-pressure membranes was higher than in intact cells (Figure 5B vs Figures 3B and 4B).

Beyond G125C on TM IV, the results obtained with intact cells were qualitatively equal to those obtained with high-pressure membranes, suggesting that the permeability barrier of the outer membrane does not limit accessibility at this TM stretch. Therefore, the results obtained from both MTSET and MTSES accessibility tests in intact cells complemented those obtained with the high-pressure membranes by adding directionality with respect to the orientation of the membrane and the NhaA funnels as follows. (a) On the basis of the crystal structure at pH 4, Cys replacements I134C−A142C were expected to be exposed to the cytoplasm but not to the periplasm. Accordingly, no MTSET accessibility was observed in intact cells at physiological pH, but high-pressure membranes exposed the cytoplasmic face of NhaA, revealing the Cys replacements that face the cytoplasm (compare Figures 3B and 5B). (b) Alkaline pH increased and acidic pH decreased the MTSET accessibility at helix IVp and the extended chain (compare Figures 5B and 3B). As discussed above, an effect of pH on the chemistry of the reaction was excluded by using Cys replacements that do not change conformation with pH.[41] Therefore, the pH effect likely reveals a pH-induced conformational change that alters the exposure of the Cys replacements

dx.doi.org/10.1021/bi301030x | *Biochemistry* 2012, 51, 9560−9569

to MTSET. In summary, when accessibility to a SH reagent is tested in a membrane protein of Gram-negative bacteria, it is important to use both high-pressure membranes and intact cells to evaluate the data.

The Crystal Structure at pH 4 Shows That Highly Conserved Residues of TM IV Line the Cytoplasmic Funnel, Are Not Exposed to Any Funnel in the Extended Chain, and Are Hardly Exposed to the Periplasmic Funnel. Aligning the NhaA TM IV protein sequence with the most recent available sequences of putative prokaryotic Na^+/H^+ antiporters (UniProt/TrEMBL databases[42]) and projecting the data (http://Consurf.tau.ac.il) on the pH 4 crystal structure[14] (Figures 1a,b and 3C) showed that the most conserved amino acid residues on helix IVc (L138, G139, and I134) are located on one face of the helix that lines the cytoplasmic funnel at pH 4 (Figure 3C). The most conserved residues of the extended chain (T132 and D133) are located below the bottom of the cytoplasmic funnel but are not exposed to any funnel[14] (Figure 3C). Some of helix IVp's residues that are embedded in the hydrophobic barrier (A131, A130, and P129) were less conserved and not exposed, but the next part of this helix (G125 and I128) was conserved and approached the periplasm at pH 4[14] (Figure 3C). The residues at both ends of TM IV, which approach the cytoplasm (L141−L143) or protrude into the periplasm (I121−E124), were only slightly conserved, if at all (Figure 3C).

Cation Passage of NhaA at Physiological pH. Because MTSET and MTSES are water-soluble, membrane-impermeant, and positively and negatively charged, respectively,[35,36] they can reach the Cys replacements exposed directly to the reaction medium or via water-filled funnels in the protein connected to the reaction medium. Furthermore, as the diameter of the positively charged MTSET is quite similar to that of hydrated Na^+, its accessibility reflects the passage of Na^+. The accessibility of the negatively charged MTSES, which is similar in size to MTSET, reflects the ability of a negative charge to penetrate this route.

Projecting the MTSET accessibility values to TM IV Cys replacements in high-pressure membranes at physiological pH (6.5 and 8.5) (Figure 5) on the pH 4 NhaA crystal structure (Figure 3C) with the conserved residues revealed some spatial differences in the Cys replacements compared to the crystal structure at pH 4. As discussed above, the accessibility of MTSET to Cys replacements in the nonconserved N-terminal tail of helix IVp [T122C−E124C (Figures 1a and 3C)] implied its localization in a periplasmic funnel at physiological pH (Figure 5A,B), like at pH 4. The accessibility of MTSET to Cys replacements in the conserved part of helix IVp (G125C−A131C) showed oscillations, as expected from the respective helix turns in the crystal structure at pH 4[14] (Figures 3C and 5). Furthermore, whereas the accessibility of MTSET to G125C and W126C was equal at both pHs, the accessibility of MTSET to the A127C−P129C stretch was ∼2-fold higher at alkaline pH than at acidic pH, implying a pH-induced conformational change (Figure 5 and see below). Similar results were obtained from the MTSET versus MTSES accessibility tests of helix IVp Cys replacements in intact cells at physiological pH, including oscillation of the accessibility and pH-dependent accessibility peaks (Figures 3B and 4B). Taken together, the results suggest that the periplasmic funnel is enlarged at physiological pH in a pH-dependent fashion, relative to its shallow depth and small size at acidic pH.[14]

According to the pH 4 crystal structure, Cys replacements A130C and A131C were expected to be embedded in the NhaA barrier separating the cytoplasmic and periplasmic funnels (ref 14 and Figure 3C). Indeed, they were barely exposed to MTSET at physiological pH in the high-pressure membranes (Figure 5B) or to either MTSET or MTSES in intact cells (Figures 3B and 4B).

Remarkably, Cys replacements of the most conserved extended chain, T132C−D133C, showed MTSET accessibility at physiological pH in high-pressure membranes that was not compatible with the crystal structure at pH 4: whereas the extended chain was not exposed to any funnel in the latter (Figure 3C), its Cys replacement D133C was 38% accessible at pH 6.5 and 95% accessible at pH 8.5 (Figure 5B), suggesting a pH-induced conformational change (see below). Similarly, the MTSET accessibility tests in intact cells revealed that D133C is highly accessible to the SH reagents, in a pH-dependent fashion, from the periplasmic funnel, with its accessibility increasing further at alkaline pH (Figure 3B). Although MTSES accessibility in intact cells was strongly reduced at the extended chain, low accessibility was found for D133C at alkaline pH (Figure 4B).

The accessibility of MTSET at physiological pH to Cys replacements in helix IVc (I134C−L143C) (Figure 3C) in high-pressure membranes reflected the crystal structure at pH 4. The Cys replacements of the most conserved residues (I134C and G139C) were highly accessible to MTSET at physiological pH (Figure 5B), and the accessibility values oscillated around these residues, reflecting the helix turns. The residues facing the opposite side of helix IVc (A135C, F136C, A137C, and V140C) were less conserved and less accessible (Figure 3C). Notably, the observed pH effect on the accessibility of MTSET to helix IVc was much smaller than that on the extended chain and helix IVp. The MTSET versus MTSES accessibility tests with helix IVc in intact cells at low and high pH were in full agreement with the pH 4 crystal structure and the results with the high-pressure membranes; except for I134C, which connects the extended chain to helix IVc, none of the Cys replacements were accessible from the periplasm to either MTSET or MTSES. Therefore, the highly conserved and MTSET-accessible residues in helix IVc are exposed to a cytoplasmic funnel, as they are in the crystal structure at pH 4.

Finally, a comparison of the MTSET and MTSES accessibility results in intact cells clearly shows that the former penetrates deeper into NhaA than the latter from the periplasmic side of the membrane (compare Figures 3 and 4). Thus, although the outer membrane serves as a stronger permeability barrier to MTSET than to MTSES at alkaline pH, MTSET reacted strongly with Cys replacements T132C−I134C at alkaline pH, whereas MTSES hardly reached D133C at physiological pH. This difference between the negatively charged MTSES and the positively charged MTSET might reflect a highly negative cytoplasmic funnel, as observed in the crystal structure at pH 4.[14]

Taken together, the cation passage, at physiological pH and pH 4, is comprised of cytoplasmic and periplasmic funnels that are lined by mostly conserved residues. However, whereas only small changes were observed in helix IVc of the cytoplasmic funnel at physiological pH, large pH-induced changes were observed at physiological pH in the extended chain and helix IVp of the periplasmic funnel, resulting in broadening of this funnel at physiological pH (see below). Accordingly, Cys

dx.doi.org/10.1021/bi301030x | *Biochemistry* 2012, 51, 9560−9569

replacements of the most conserved residues in helix IVp, the extended chain, and helix IVc that line the putative cation passage at physiological pH increased the apparent K_m of the antiporter activity to both Na^+ and Li^+ at physiological pH (Figure 1b and Table 1).

The Extended Chain and Adjacent Helix IVp Are Involved in a Strong pH-Induced Conformational Change between pH 6.5 and 8.5. Our tests of the accessibility of both MTSET and MTSES to TM IV in intact cells (Figures 3 and 4) and of MTSET in high-pressure membranes (Figure 5) revealed that whereas helix IVc hardly changes its conformation with pH, a large alkaline pH-induced conformational change is observed in the extended chain and the adjacent residues in helix IVp. In line with the pH-induced conformational change at helix IVp, two Cys replacements [G125C[34] and A131C (Figure 2B)] were found to affect the pH response of NhaA.

Furthermore, cryo-electron microscopy of two-dimensional crystals obtained at acidic pH and soaked at alkaline pH in the presence and absence of Na^+ revealed a Na^+-induced conformational change of NhaA helix IVp.[43] We could not determine the accessibility to MTSET in the absence of Na^+ because most of the reagents were not Na^+-free. However, previous computational analysis of NhaA also showed that helix IVp changes conformation with pH.[44]

The pronounced pH-induced conformational change revealed here at the extended chain has never before been observed. Cys replacements of the conserved residues in the extended chain, T132C and D133C, and in its vicinity, I134C, become exposed to the periplasm in a pH-dependent manner. In line with this result, we previously identified a pH-induced conformational change at physiological pH in the N-terminal part of helix VIc using Trp replacement F136W.[39]

Many results (reviewed in ref 45) have shown that Cys replacements of residues in NhaA that change conformation with pH also impair the pH response of the antiporter. However, although an important role has been suggested for D133 of the extended chain in NhaA's pH response,[19] Cys replacements of residues T132 and D133 have been shown to strongly affect the apparent K_m of NhaA without affecting its pH response[34] (Table 1). Moreover, as shown here, most other Cys replacements in TM IV affect the apparent K_m of NhaA but not its pH response (Table 1 and Figures 1b and 2). Interestingly, similar results were obtained with HpNhaA, a close homologue of NhaA from *Helicobacter pylori*.[46] Therefore, we cannot exclude the possibility that the pH-induced change in accessibility seen here at the extended chain is not due to its movement but rather to a conformational change in a neighboring helix or in another extended chain (TM XI) nearby (Figure 1). Modeling of the open conformation of NhaA at alkaline pH has shown alkaline pH-induced opening of a pathway from the periplasm toward the extended chain.[47] Such an opening might account for the alkaline pH-induced accessibility of MTSET to Cys replacement(s) in the extended chain without being itself part of NhaA's pH response.

AUTHOR INFORMATION

Corresponding Author

*Department of Biological Chemistry, Alexander Silberman Institute of Life Sciences, Hebrew University of Jerusalem, 91904 Jerusalem, Israel. Phone: 972-2-6585094. Fax: 972-2-6586947. E-mail: etana@vms.huji.ac.il.

Funding

This research was supported by EDICT (EU FP 7, European Drug Initiative on Channels and Transporters), the United States-Israel Binational Science Foundation (BSF, 501/03-16.2), and the Israel Science Foundation (Grant 284/12) to E.P.

Notes

The authors declare no competing financial interest.

ABBREVIATIONS

TM, transmembrane segment; CL-NhaA, cysteine-less NhaA; MTSES, 2-sulfonatoethyl methanethiosulfonate; MTSET, [2-(trimethylammonium)ethyl] methanethiosulfonate bromide.

REFERENCES

(1) Padan, E., Venturi, M., Gerchman, Y., and Dover, N. (2001) Na^+/H^+ antiporters. *Biochim. Biophys. Acta 1505*, 144−157.

(2) Padan, E., Bibi, E., Masahiro, I., and Krulwich, T. A. (2005) Alkaline pH homeostasis in bacteria: New insights. *Biochim. Biophys. Acta 1717*, 67−88.

(3) Padan, E. (2008) The enlightening encounter between structure and function in the NhaA Na^+-H^+ antiporter. *Trends Biochem. Sci. 33*, 435−443.

(4) Fliegel, L. (2008) Molecular biology of the myocardial Na^+/H^+ exchanger. *J. Mol. Cell. Cardiol. 44*, 228−237.

(5) Pinner, E., Kotler, Y., Padan, E., and Schuldiner, S. (1993) Physiological role of *nhaB*, a specific Na^+/H^+ antiporter in *Escherichia coli*. *J. Biol. Chem. 268*, 1729−1734.

(6) Brett, C. L., Donowitz, M., and Rao, R. (2005) Evolutionary origins of eukaryotic sodium/proton exchangers. *Am. J. Physiol. 288*, C223−C239.

(7) Taglicht, D., Padan, E., and Schuldiner, S. (1991) Overproduction and purification of a functional Na^+/H^+ antiporter coded by *nhaA* (*ant*) from *Escherichia coli*. *J. Biol. Chem. 266*, 11289−11294.

(8) Taglicht, D., Padan, E., and Schuldiner, S. (1993) Proton-sodium stoichiometry of NhaA, an electrogenic antiporter from *Escherichia coli*. *J. Biol. Chem. 268*, 5382−5387.

(9) Orlowski, J. a. G., S. (2003) Molecular and Functional Diversity of Mammalian Na^+/H^+ Exchangers. In *The Sodium Hydrogen Exchange, from Molecule to its Role in Disease* (Karmazin, M., Avkiran, N., and Fliegel, L., Eds.) pp 17−34, Kluwer Academic Publishers, Boston.

(10) Orlowski, J., and Grinstein, S. (2004) Diversity of the mammalian sodium/proton exchanger SLC9 gene family. *Pfluegers Arch. 447*, 549−565.

(11) Putney, L. K., Denker, S. P., and Barber, D. L. (2002) The changing face of the Na^+/H^+ exchanger, NHE1: Structure, regulation, and cellular actions. *Annu. Rev. Pharmacol. Toxicol. 42*, 527−552.

(12) Wakabayashi, S., Hisamitsu, T., Pang, T., and Shigekawa, M. (2003) Kinetic dissection of two distinct proton binding sites in Na^+/H^+ exchangers by measurement of reverse mode reaction. *J. Biol. Chem. 278*, 43580−43585.

(13) Orlowski, J., and Grinstein, S. (2007) Emerging roles of alkali cation/proton exchangers in organellar homeostasis. *Curr. Opin. Cell Biol. 19*, 483−492.

(14) Hunte, C., Screpanti, M., Venturi, M., Rimon, A., Padan, E., and Michel, H. (2005) Structure of a Na^+/H^+ antiporter and insights into mechanism of action and regulation by pH. *Nature 534*, 1197−1202.

(15) Padan, E., Kozachkov, L., Herz, K., and Rimon, A. (2009) NhaA crystal structure: Functional-structural insights. *J. Exp. Biol. 212*, 1593−1603.

(16) Krishnamurthy, H., Piscitelli, C. L., and Gouaux, E. (2009) Unlocking the molecular secrets of sodium-coupled transporters. *Nature 459*, 347−355.

(17) Boudker, O., and Verdon, G. (2010) Structural perspectives on secondary active transporters. *Trends Pharmacol. Sci. 31*, 418−426.

(18) Hu, N. J., Iwata, S., Cameron, A. D., and Drew, D. (2011) Crystal structure of a bacterial homologue of the bile acid sodium symporter ASBT. *Nature 478*, 408−411.
(19) Arkin, I. T., Xu, H., Jensen, M. O., Arbely, E., Bennett, E. R., Bowers, K. J., Chow, E., Dror, R. O., Eastwood, M. P., Flitman-Tene, R., Gregersen, B. A., Klepeis, J. L., Kolossvary, I., Shan, Y., and Shaw, D. E. (2007) Mechanism of Na^+/H^+ antiporting. *Science 317*, 799−803.
(20) Padan, E., Maisler, N., Taglicht, D., Karpel, R., and Schuldiner, S. (1989) Deletion of *ant* in *Escherichia coli* reveals its function in adaptation to high salinity and an alternative Na^+/H^+ antiporter system(s). *J. Biol. Chem. 264*, 20297−20302.
(21) Davies, B., and Mingioli, E. (1950) Mutants of *Escherichia coli* requiring methionine or vitamin B12. *J. Bacteriol. 60*, 17−28.
(22) Galili, L., Rothman, A., Kozachkov, L., Rimon, A., and Padan, E. (2002) Transmembrane domain IV is involved in ion transport activity and pH regulation of the NhaA-Na^+/H^+ antiporter of *Escherichia coli*. *Biochemistry 41*, 609−617.
(23) Ho, S. N., Hunt, H. D., Horton, R. M., Pullen, J. K., and Pease, L. R. (1989) Site-directed mutagenesis by overlap extension using the polymerase chain reaction. *Gene 77*, 51−59.
(24) Fisher, C. L., and Pei, G. K. (1997) Modification of a PCR-based site-directed mutagenesis method. *BioTechniques 23*, 570−574.
(25) Rimon, A., Tzubery, T., Galili, L., and Padan, E. (2002) Proximity of cytoplasmic and periplasmic loops in NhaA Na^+/H^+ antiporter of *Escherichia coli* as determined by site-directed thiol cross-linking. *Biochemistry 41*, 14897−14905.
(26) Gerchman, Y., Olami, Y., Rimon, A., Taglicht, D., Schuldiner, S., and Padan, E. (1993) Histidine-226 is part of the pH sensor of NhaA, a Na^+/H^+ antiporter in *Escherichia coli*. *Proc. Natl. Acad. Sci. U.S.A. 90*, 1212−1216.
(27) Rosen, B. P. (1986) Ion extrusion systems in *E. coli*. *Methods Enzymol. 125*, 328−386.
(28) Goldberg, E. B., Arbel, T., Chen, J., Karpel, R., Mackie, G. A., Schuldiner, S., and Padan, E. (1987) Characterization of a Na^+/H^+ antiporter gene of *Escherichia coli*. *Proc. Natl. Acad. Sci. U.S.A. 84*, 2615−2619.
(29) Schuldiner, S., and Fishkes, H. (1978) Sodium-proton antiport in isolated membrane vesicles of *Escherichia coli*. *Biochemistry 17*, 706−711.
(30) Tsuboi, Y., Inoue, H., Nakamura, N., and Kanazawa, H. (2003) Identification of membrane domains of the Na^+/H^+ antiporter (NhaA) protein from *Helicobacter pylori* required for ion transport and pH sensing. *J. Biol. Chem. 278*, 21467−21473.
(31) Bradford, M. M. (1976) A rapid and sensitive method for the quantitation of microgram quantities of protein utilizing the principle of protein-dye binding. *Anal. Biochem. 72*, 248−254.
(32) Olami, Y., Rimon, A., Gerchman, Y., Rothman, A., and Padan, E. (1997) Histidine 225, a residue of the NhaA-Na^+/H^+ antiporter of *Escherichia coli* is exposed and faces the cell exterior. *J. Biol. Chem. 272*, 1761−1768.
(33) Rimon, A., Gerchman, Y., Kariv, Z., and Padan, E. (1998) A point mutation (G338S) and its suppressor mutations affect both the pH response of the NhaA-Na^+/H^+ antiporter as well as the growth phenotype of *Escherichia coli*. *J. Biol. Chem. 273*, 26470−26476.
(34) Galili, L., Herz, K., Dym, O., and Padan, E. (2004) Unraveling functional and structural interactions between transmembrane domains IV and XI of NhaA Na^+/H^+ antiporter of *Escherichia coli*. *J. Biol. Chem. 279*, 23104−23113.
(35) Akabas, M. H., Kaufmann, C., Archdeacon, P., and Karlin, A. (1994) Identification of acetylcholine receptor channel-lining residues in the entire M2 segment of the α subunit. *Neuron 13*, 919−927.
(36) Akabas, M. H., Stauffer, D. A., Xu, M., and Karlin, A. (1992) Acetylcholine receptor channel structure probed in cysteine-substitution mutants. *Science 258*, 307−310.
(37) Diab, M., Rimon, A., Tzubery, T., and Padan, E. (2011) Helix VIII of NhaA Na^+/H^+ antiporter participates in the periplasmic cation passage and pH regulation of the antiporter. *J. Mol. Biol. 413*, 604−614.
(38) Guan, L., and Kaback, H. R. (2007) Site-directed alkylation of cysteine to test solvent accessibility of membrane proteins. *Nat. Protoc. 2*, 2012−2017.
(39) Kozachkov, L., and Padan, E. (2011) Site-directed tryptophane fluorescence reveals two essential conformational changes in the Na^+/H^+ antiporter NhaA. *Proc. Natl. Acad Sci. USA 108*, 15769−15774.
(40) Tzubery, T., Rimon, A., and Padan, E. (2008) Structure-based functional study reveals multiple roles of transmembrane segment IX and loop VIII-IX in NhaA Na^+/H^+ antiporter of *Escherichia coli* at physiological pH. *J. Biol. Chem. 283*, 15975−15987.
(41) Herz, K., Rimon, A., Olkhova, E., Kozachkov, L., and Padan, E. (2010) Transmembrane segment II of NhaA Na^+/H^+ antiporter lines the cation passage, and Asp65 is critical for pH activation of the antiporter. *J. Biol. Chem. 285*, 2211−2220.
(42) Combet, C., Blanchet, C., Geourjon, C., and Deleage, G. (2000) NPS@: Network protein sequence analysis. *Trends Biochem. Sci. 25*, 147−150.
(43) Appel, M., Hizlan, D., Vinothkumar, K. R., Ziegler, C., and Kuhlbrandt, W. (2009) Conformations of NhaA, the Na/H exchanger from *Escherichia coli*, in the pH-activated and ion-translocating states. *J. Mol. Biol. 386*, 351−365.
(44) Olkhova, E., Padan, E., and Michel, H. (2007) The influence of protonation states on the dynamics of the NhaA antiporter from *Escherichia coli*. *Biophys. J. 92*, 3784−3791.
(45) Padan, E. A., and Kozachkov, L. (2012) Conformational changes in NhaA Na^+/H^+ antiporter. *Mol. Membr. Biol.*, in press.
(46) Kuwabara, N., Inoue, H., Tsuboi, Y., Nakamura, N., and Kanazawa, H. (2004) The fourth transmembrane domain of the *Helicobacter pylori* Na^+/H^+ antiporter NhaA faces a water-filled channel required for ion transport. *J. Biol. Chem. 279*, 40567−40575.
(47) Schushan, M., Rimon, A., Haliloglu, T., Forrest, L. R., Padan, E., and Ben-Tal, N. (2012) A Model-Structure of a Periplasm-facing State of the NhaA Antiporter Suggests the Molecular Underpinnings of pH-induced Conformational Changes. *J. Biol. Chem. 287*, 18249−18261.